Appl. Math. Mech. -Engl. Ed., **39**(5), 685–702 (2018)

Applied Mathematics and Mechanics (English Edition)

https://doi.org/10.1007/s10483-018-2325-6

One-dimensional dynamic equations of a piezoelectric semiconductor beam with a rectangular cross section and their application in static and dynamic characteristic analysis*

Peng LI[1], Feng JIN[2,†], Jianxun MA[1]

1. School of Human Settlements and Civil Engineering, Xi'an Jiaotong University, Xi'an 710049, China;
2. State Key Laboratory for Strength and Vibration of Mechanical Structures, Xi'an Jiaotong University, Xi'an 710049, China

(Received Jul. 8, 2017 / Revised Sept. 18, 2017)

Abstract Within the framework of continuum mechanics, the double power series expansion technique is proposed, and a series of reduced one-dimensional (1D) equations for a piezoelectric semiconductor beam are obtained. These derived equations are universal, in which extension, flexure, and shear deformations are all included, and can be degenerated to a number of special cases, e.g., extensional motion, coupled extensional and flexural motion with shear deformations, and elementary flexural motion without shear deformations. As a typical application, the extensional motion of a ZnO beam is analyzed sequentially. It is revealed that semi-conduction has a great effect on the performance of the piezoelectric semiconductor beam, including static deformations and dynamic behaviors. A larger initial carrier density will evidently lead to a lower resonant frequency and a smaller displacement response, which is a little similar to the dissipative effect. Both the derived approximate equations and the corresponding qualitative analysis are general and widely applicable, which can clearly interpret the inner physical mechanism of the semiconductor in the piezoelectrics and provide theoretical guidance for further experimental design.

Key words piezoelectric semiconductor beam, reduced one-dimensional (1D) equation, double power series expansion technique, stress relaxation, initial carrier density

Chinese Library Classification O343.8
2010 Mathematics Subject Classification 74H45

* Citation: Li, P., Jin, F., and Ma, J. X. One-dimensional dynamic equations of a piezoelectric semiconductor beam with a rectangular cross section and their application in static and dynamic characteristic analysis. *Applied Mathematics and Mechanics* (*English Edition*), **39**(5), 685–702 (2018) https://doi.org/10.1007/s10483-018-2325-6

† Corresponding author, E-mail: jinfengzhao@263.net

Project supported by the National Natural Science Foundation of China (Nos. 11672223, 11402187, and 51178390), the China Postdoctoral Science Foundation (No. 2014M560762), and the Fundamental Research Funds for the Central Universities of China (No. xjj2015131)

1 Introduction

Owing to their capacity of facilitating the conversion between mechanical and electric energies, piezoelectric materials have been manufactured into various kinds of surface acoustic wave (SAW) and bulk acoustic wave (BAW) devices[1–6], e.g., actuators and sensors for wave generation and reception[2–3], transformers for raising or lowering voltages[4], energy harvesters for energy conversion and handling[5], and gyroscopes for detecting the vibration of moving objects[6]. During the past decades, many efforts have been concentrated on the inner physical and mechanical properties of these piezoelectric devices, including temperature stability[7], initial bias[8], material coefficient inhomogeneity[9], dissipation[10], viscous effect[11], and large deformation and nonlinearity[5]. Simplifying piezoelectric materials into dielectrics (insulators) is a well-known theoretical methodology[12], in which small electrical conduction is usually ignored. Generally, no real material can be considered as perfect insulators[13], since all existing materials show certain levels of electrical conduction. Therefore, the zero charge equation of electrostatics and boundary conditions has been improved[14], which can effectively simulate the effect of real current. It has been revealed that low ohmic conduction and related dissipative effects should also be considered in quartz crystals, which are usually treated as good insulators, especially when the Q values (quality factor) of these devices are calculated[14]. To some extent, the effect of semi-conduction on the performance of piezoelectric devices is unknown, which is just the origin of the present contribution. Hence, in the present work, we consider the piezoelectric semiconductor beam as a research target, and discuss its basic mechanical and physical behaviors to reveal the semiconduction effect on the behaviors of piezoelectric materials.

As we know, piezoelectric materials belong to anisotropic media, and extension may induce mechanical deformations, e.g., flexure, shear, and torsion. The deformation in piezoelectric materials is very complex, and the static and dynamic properties are difficult to be analyzed. Even for an infinite plate or a finite beam, few exact solutions can be obtained theoretically at present. In other words, classical three-dimensional (3D) equations are difficult to be used in the direct analysis of single vibration modes[15], and improvement or approximation should be provided[16–17]. Hence, under the framework of continuum mechanics, we will propose a double power series expansion technique in this paper to derive the approximate one-dimensional (1D) equations of a piezoelectric semiconductor beam. Some necessary stress relaxation relations are introduced, and the extension, flexure, and shear constitutive relations are revised correspondingly. For piezoelectric semiconductor materials, the carrier diffusion not only contributes to the current, but also contributes to the carrier drift under an electric field associated with the ohmic conduction[18]. The current boundary condition is rewritten. Based on the derived equations, the extensional motion of a ZnO beam is considered as the numerical simulation, and the effect of the initial carrier density on the extensional behavior is discussed in detail. The theoretical equations and numerical outcome are general, which can clearly interpret the inner physical mechanism of the semiconductors in the piezoelectrics and provide theoretical guidance for further experimental design of piezoelectric semiconductor devices.

2 Basic 3D equations

Similar to piezoelectrics, the basic coupled electro-mechanical behavior of piezoelectric semiconductors can be analyzed theoretically in the framework of continuum mechanics[19–20]. We consider a homogeneous one-carrier piezoelectric semiconductor under a uniform direct current (DC) electric field $\overline{E}_j$ with the carrier charge q and the initial steady state carrier density $\overline{n}$. In the linear theory of piezoelectricity, the corresponding displacement component u_i, electrical potential function φ, and perturbation of the carrier density n should, respectively, satisfy Newton's law, Gauss's law of electrostatics, and the conservation of charge[18–20].

$$T_{ij,j} + \rho f_i = \rho \ddot{u}_i, \quad D_{i,i} = qn, \quad q\dot{n} + J_{i,i} = 0, \tag{1}$$

where T_{ij}, D_i, and J_i denote the components of the stress, the electric field, and the electric current, respectively. ρ is the mass density, and f_i is the body force per unit mass. A superimposed dot represents differentiation with respect to the time t. The summation convention for repeated tensor indices is used. Equations (2) and (3) are only suitable for positive holes, which are just as an example in the present contribution. From the mathematical view, if electrons are considered, the two equations are still applicable after n (or q) is replaced by $-n$ (or $-q$). The generalized constitutive relations of piezoelectric semiconductors are[18–20]

$$S_{ij} = s_{ijkl}T_{kl} + e_{kij}E_k, \quad D_i = e_{ikl}T_{kl} + \varepsilon_{ik}E_k, \quad J_i = q\overline{n}\mu_{ij}E_j + qn\mu_{ij}\overline{E}_j - qd_{ij}N_j, \tag{2}$$

where s_{ijkl} and e_{kij} represent the elastic compliances, ε_{ik} is the piezoelectric constant, μ_{ij} is the dielectric permittivity, and d_{ij} represents the diffusion constant. For electrons, Eq. (2) should be improved as follows:

$$J_i = q\overline{n}\mu_{ij}E_j + qn\mu_{ij}\overline{E}_j + qd_{ij}N_j.$$

Here, the strain tensor S_{ij}, electric field E_i, and carrier density gradient N_i are, respectively, defined by

$$S_{ij} = \frac{1}{2}(u_{i,j} + u_{j,i}), \quad E_i = -\varphi_{,i}, \quad N_i = n_{,i}. \tag{3}$$

In order to solve the above differential equations, necessary boundary conditions should be adopted. If the unit outward normal vector of the boundary is denoted by ζ, the mechanical displacement component u_i or the traction vector $T_{ij}\zeta_j$, the electric potential function φ or the normal component of the electric displacement vector $D_i\zeta_i$, and the carrier density n or the normal current $J_i\zeta_i$ may be prescribed to obtain the closed-form solution to the problem[21]. The boundary condition containing the normal current $J_i\zeta_i$ should be improved into $\zeta_i(\dot{D}_i + J_i)$ for the piezoelectric semiconductor[12].

3 Double power series expansion technique

The considered piezoelectric semiconductor beam with a rectangular cross section is shown in Fig. 1, where the length is much larger than the width and thickness, i.e., $c \gg a$, b. Under this condition, the reduced 1D equations for the piezoelectric semiconductor beam can be derived with the mechanical displacement component u_i, electrical potential function φ, and perturbation of the carrier density n written by the following double power series expansions[22–25]:

$$\begin{cases} u_i = \displaystyle\sum_{m,p=0}^{\infty} x_1^m x_2^p u_i^{(m,p)}(x_3,t), \\ \varphi = \displaystyle\sum_{m,p=0}^{\infty} x_1^m x_2^p \varphi^{(m,p)}(x_3,t), \\ n = \displaystyle\sum_{m,p=0}^{\infty} x_1^m x_2^p n^{(m,p)}(x_3,t). \end{cases} \tag{4}$$

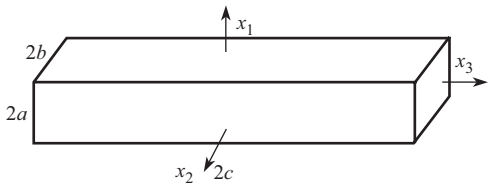

Fig. 1 Theoretical model of a piezoelectric semiconductor beam with a rectangular cross section

It should be stressed here that, the full mechanical properties of the piezoelectric semiconductor beam have been included by the expansions in Eq. (4) and the general derivation. Some particular motion for extension can be deduced from this expression. For example, the usual zeroth-order theory can be obtained easily when the series is truncated with only one term, i.e., $m = p = 0$. The first-order theory for the coupled extensional and flexural motion corresponds to the cases where m and p are smaller than 2. Similarly, the related higher-order theory with larger m and p, which could depict various deformations of the cross section, can also be captured[23–25]. Based on the double power series, the corresponding strain tensor S_{ij}, electric field E_i, and carrier density gradient N_i in Eq. (3) can be written as follows:

$$S_{ij} = \sum_{m,p=0}^{\infty} x_1^m x_2^p S_{ij}^{(m,p)}, \quad E_i = \sum_{m,p=0}^{\infty} x_1^m x_2^p E_i^{(m,p)}, \quad N_i = \sum_{m,p=0}^{\infty} x_1^m x_2^p N_i^{(m,p)}, \tag{5}$$

where

$$\begin{cases} S_{ij}^{(m,p)} = \dfrac{1}{2}(u_{i,j}^{(m,p)} + u_{j,i}^{(m,p)}) + (m+1)(\delta_{1i}u_j^{(m+1,p)} + \delta_{1j}u_i^{(m+1,p)}) \\ \qquad\qquad + (p+1)(\delta_{2i}u_j^{(m,p+1)} + \delta_{2j}u_i^{(m,p+1)}), \\ E_i^{(m,p)} = -\varphi_{,i}^{(m,p)} - (m+1)\delta_{1i}\varphi_i^{(m+1,p)} - (p+1)\delta_{2i}\varphi_i^{(m,p+1)}, \\ N_i^{(m,p)} = n_{,i}^{(m,p)} + (m+1)\delta_{1i}n_i^{(m+1,p)} + (p+1)\delta_{2i}n_i^{(m,p+1)}. \end{cases} \tag{6}$$

Correspondingly, the generalized constitutive relations of the piezoelectric semiconductors can be expressed as follows:

$$\begin{cases} \displaystyle\sum_{r,s=0}^{\infty} A_{(mprs)}S_{ij}^{(r,s)} = s_{ijkl}T_{kl}^{(m,p)} + \sum_{r,s=0}^{\infty} A_{(mprs)}e_{kij}E_k^{(r,s)}, \\ \\ \displaystyle D_i^{(m,p)} = e_{ikl}T_{kl}^{(m,p)} + \sum_{r,s=0}^{\infty} A_{(mprs)}\varepsilon_{ik}E_k^{(r,s)}, \\ \\ \displaystyle J_i^{(m,p)} = q\sum_{r,s=0}^{\infty} A_{(mprs)}(\overline{n}\mu_{ij}E_j^{(r,s)} + \mu_{ij}\overline{E}_j n^{(r,s)} - d_{ij}N_j^{(r,s)}), \end{cases} \tag{7}$$

where the stress resultant $T_{ij}^{(m,p)}$, electric displacement resultant $D_i^{(m,p)}$, and electric current resultant $J_i^{(m,p)}$ are, respectively, defined by

$$T_{ij}^{(m,p)} = \int_A T_{ij}x_1^m x_2^p \mathrm{d}A, \quad D_i^{(m,p)} = \int_A D_i x_1^m x_2^p \mathrm{d}A, \quad J_i^{(m,p)} = \int_A J_i x_1^m x_2^p \mathrm{d}A. \tag{8}$$

In the above equations, $A = 4ab$ is the area of the cross section, and

$$A_{(mprs)} = \int_A x_1^{m+r}x_2^{p+s}\mathrm{d}A = \begin{cases} \dfrac{4a^{m+r+1}b^{p+s+1}}{(m+r+1)(p+s+1)}, & m+r \text{ and } p+s \text{ are even}, \\ 0, \quad \text{else}. \end{cases} \tag{9}$$

Multiplying Eq. (1) by $x_1^m x_2^p$ and integrating, we can obtain the final 1D governing equations as follows[16–18,22–25]:

$$\begin{cases} T_{3i,3}^{(m,p)} - mT_{1i}^{(m-1,p)} - pT_{2i}^{(m,p-1)} + F_i^{(m,p)} = \rho \sum\limits_{r,s=0}^{\infty} A_{(mprs)} \ddot{u}_i^{(r,s)}, \\ D_{3,3}^{(m,p)} - mD_1^{(m-1,p)} - pD_2^{(m,p-1)} + D^{(m,p)} = q \sum\limits_{r,s=0}^{\infty} A_{(mprs)} n^{(r,s)}, \\ q \sum\limits_{r,s=0}^{\infty} A_{(mprs)} \dot{n}^{(r,s)} + J_{3,3}^{(m,p)} - mJ_1^{(m-1,p)} - pJ_2^{(m,p-1)} + J^{(m,p)} = 0, \end{cases} \tag{10}$$

where

$$F_i^{(m,p)} = T_i^{(m,p)} + \rho f_i^{(m,p)}, \quad f_i^{(m,p)} = \int_A f_i x_1^m x_2^p \mathrm{d}A.$$

Meanwhile, the corresponding surface traction resultant $T_i^{(m,p)}$, electric displacement resultant $D^{(m,p)}$, and electric current resultant $J^{(m,p)}$ of various orders are

$$\begin{cases} T_i^{(m,p)} = a^m \displaystyle\int_{-b}^{b} \Big(T_{1i}(a) - (-1)^m T_{1i}(-a)\Big) x_2^p \mathrm{d}x_2 \\ \qquad\qquad + b^p \displaystyle\int_{-a}^{a} \Big(T_{2i}(b) - (-1)^p T_{2i}(-b)\Big) x_1^m \mathrm{d}x_1, \\ D^{(m,p)} = a^m \displaystyle\int_{-b}^{b} \Big(D_1(a) - (-1)^m D_1(-a)\Big) x_2^p \mathrm{d}x_2 \\ \qquad\qquad + b^p \displaystyle\int_{-a}^{a} \Big(D_2(b) - (-1)^p D_2(-b)\Big) x_1^m \mathrm{d}x_1, \\ J^{(m,p)} = a^m \displaystyle\int_{-b}^{b} \Big(J_1(a) - (-1)^m J_1(-a)\Big) x_2^p \mathrm{d}x_2 \\ \qquad\qquad + b^p \displaystyle\int_{-a}^{a} \Big(J_2(b) - (-1)^p J_2(-b)\Big) x_1^m \mathrm{d}x_1. \end{cases} \tag{11}$$

4 1D theory for the piezoelectric semiconductor beam

Corresponding to different truncations of the double power series, different cases degenerated from the 1D theory will be introduced and explained in detail in the following content.

4.1 Zeroth-order theory for extension

The zeroth-order theory for extension can be deduced easily when the series is truncated with only one term, i.e., $m = p = 0$. It is valid when the concerned wavelength is much larger than the dimensions of the rectangular cross section[26]. The main characteristics of the beam will be controlled by $u_3^{(0,0)}$, $\varphi^{(0,0)}$, and $n^{(0,0)}$. The major strain component is

$$S_3 = S_{33} = u_{3,3}^{(0,0)}. \tag{12}$$

Considering the Poisson effect, other zeroth-order strain components cannot be set to zero. Nevertheless, they will be eliminated instead. This process is taken as the stress relaxation

procedure[16,18,24–26]. For convenience, the usual compact matrix notation[24] with $u, v = 1, 2, \cdots, 6$ will be adopted, so that Eq. (7) can be written as follows:

$$A_{(0000)}S_u^{(0,0)} = s_{uv}T_v^{(0,0)} + A_{(0000)}e_{ku}E_k^{(0,0)}, \tag{13}$$

$$D_i^{(0,0)} = e_{iu}T_u^{(0,0)} + A_{(0000)}\varepsilon_{ik}E_k^{(0,0)}, \tag{14}$$

$$J_i^{(0,0)} = qA_{(0000)}(\overline{n}\mu_{ij}E_j^{(0,0)} + \mu_{ij}\overline{E}_j n^{(0,0)} - d_{ij}N_j^{(0,0)}), \tag{15}$$

where $A_{(0000)} = A = 4ab$. Meanwhile, considering that the extension of the beam is mainly represented by the major stress $T_3^{(0,0)}$ and the beam features a slender shape with $c \gg a, b$, we can set[16,18,24–25]

$$T_1^{(0,0)} = T_2^{(0,0)} = T_4^{(0,0)} = T_5^{(0,0)} = T_6^{(0,0)} = 0, \tag{16}$$

which is just the stress relaxation condition. Then, the expression of $T_3^{(0,0)}$ can be degenerated from Eq. (13), i.e.,

$$T_3^{(0,0)} = 4ab(\widetilde{c}_{33}S_3^{(0,0)} - \widetilde{e}_{k3}E_k^{(0,0)}), \tag{17}$$

where

$$\widetilde{c}_{33} = \frac{1}{s_{33}}, \quad \widetilde{e}_{k3} = \frac{e_{k3}}{s_{33}}.$$

Furthermore, the corresponding zeroth-order constitutive relations governing $D_i^{(0,0)}$ and $J_i^{(0,0)}$ can be obtained via Eqs. (13)–(17) as follows:

$$D_i^{(0,0)} = 4ab(\widetilde{e}_{i3}S_3^{(0,0)} + \widetilde{\varepsilon}_{ik}E_k^{(0,0)}), \tag{18}$$

$$J_i^{(0,0)} = 4abq(\overline{n}\mu_{ij}E_j^{(0,0)} + \mu_{ij}\overline{E}_j n^{(0,0)} - d_{ij}N_j^{(0,0)}), \tag{19}$$

where

$$\widetilde{\varepsilon}_{ik} = \varepsilon_{ik} - \frac{e_{i3}e_{k3}}{s_{33}}.$$

On the basis of stress relaxation, the final governing equations for the zeroth-order theory of the piezoelectric semiconductor beam (see Fig. 1) can be summarized as follows:

$$T_{33,3}^{(0,0)} + F_3^{(0,0)} = 4ab\rho\ddot{u}_3^{(0,0)}, \tag{20}$$

$$D_{3,3}^{(0,0)} + D^{(0,0)} = 4abqn^{(0,0)}, \tag{21}$$

$$4abq\dot{n}^{(0,0)} + J_{3,3}^{(0,0)} + J^{(0,0)} = 0. \tag{22}$$

To obtain the closed-form solutions, $u_3^{(0,0)}$ or $T_3^{(0,0)}$, $\varphi^{(0,0)}$ or $D_3^{(0,0)}$, and $n^{(0,0)}$ or $(\dot{D}_3^{(0,0)} + J_3^{(0,0)})$ need to be prescribed at the end of $x_3 = \pm c$.

4.2 First-order theory for the coupled extensional and flexural motions

Actually, if a finite piezoelectric semiconductor beam suffers from the external homogeneous pressure, extensional motion will occur, accompanied with inevitable flexural and torsional deformations. This is due to the anisotropy of the material. The piezoelectric semiconductor beam shown in Fig. 1 is transversely isotropic with the polarization along the z-axis, and does

not exhibit coupling to torsional modes[24–25]. Therefore, the aforementioned equations can be reduced to a first-order theory for coupled extensional and flexural motion without torsion. In this case, the equations containing extension ($u_3^{(0,0)}$), flexure ($u_1^{(0,0)}$ and $u_2^{(0,0)}$), and shear deformations ($u_3^{(1,0)}$ and $u_3^{(0,1)}$) with electrical potential functions ($\varphi^{(0,0)}$, $\varphi^{(1,0)}$, and $\varphi^{(0,1)}$) and the perturbation of the carrier density ($n^{(0,0)}$, $n^{(1,0)}$, and $n^{(0,1)}$) can be retained from Eq. (10) as follows:

$$T_{33,3}^{(0,0)} + F_3^{(0,0)} = 4ab\rho\ddot{u}_3^{(0,0)}, \tag{23}$$

$$\begin{cases} T_{31,3}^{(0,0)} + F_1^{(0,0)} = 4ab\rho\ddot{u}_1^{(0,0)}, \\ T_{32,3}^{(0,0)} + F_2^{(0,0)} = 4ab\rho\ddot{u}_2^{(0,0)}. \end{cases} \tag{24}$$

$$\begin{cases} T_{33,3}^{(1,0)} - T_{13}^{(0,0)} + F_3^{(1,0)} = \dfrac{4}{3}a^3b\rho\ddot{u}_3^{(1,0)}, \\ T_{33,3}^{(0,1)} - T_{23}^{(0,0)} + F_3^{(0,1)} = \dfrac{4}{3}ab^3\rho\ddot{u}_3^{(0,1)}. \end{cases} \tag{25}$$

$$\begin{cases} D_{3,3}^{(0,0)} + D^{(0,0)} = 4abqn^{(0,0)}, \\ D_{3,3}^{(1,0)} - D_1^{(0,0)} + D^{(1,0)} = \dfrac{4}{3}a^3bqn^{(1,0)}, \\ D_{3,3}^{(0,1)} - D_2^{(0,0)} + D^{(0,1)} = \dfrac{4}{3}ab^3qn^{(0,1)}. \end{cases} \tag{26}$$

$$\begin{cases} 4abq\dot{n}^{(0,0)} + J_{3,3}^{(0,0)} + J^{(0,0)} = 0, \\ \dfrac{4}{3}a^3bq\dot{n}^{(1,0)} + J_{3,3}^{(1,0)} - J_1^{(0,0)} + J^{(1,0)} = 0, \\ \dfrac{4}{3}ab^3q\dot{n}^{(0,1)} + J_{3,3}^{(0,1)} - J_2^{(0,0)} + J^{(0,1)} = 0. \end{cases} \tag{27}$$

The corresponding strain components and electric fields of various orders are, respectively, stated as follows:

$$S_{33}^{(0,0)} = u_{3,3}^{(0,0)}, \quad 2S_{31}^{(0,0)} = u_{1,3}^{(0,0)} + u_3^{(1,0)}, \quad 2S_{32}^{(0,0)} = u_{2,3}^{(0,0)} + u_3^{(0,1)}, \tag{28}$$

$$S_{33}^{(1,0)} = u_{3,3}^{(1,0)}, \quad S_{33}^{(0,1)} = u_{3,3}^{(0,1)}, \tag{29}$$

$$E_3^{(0,0)} = -\varphi_{,3}^{(0,0)}, \quad E_1^{(0,0)} = -\varphi^{(1,0)}, \quad E_2^{(0,0)} = -\varphi^{(0,1)}, \tag{30}$$

$$E_3^{(1,0)} = -\varphi_{,3}^{(1,0)}, \quad E_3^{(0,1)} = -\varphi_{,3}^{(0,1)}. \tag{31}$$

Similarly, the relevant zeroth- and first-order gradients of the carrier density are stated, respectively, as follows:

$$N_3^{(0,0)} = n_{,3}^{(0,0)}, \quad N_1^{(0,0)} = n^{(1,0)}, \quad N_2^{(0,0)} = n^{(0,1)}, \tag{32}$$

$$N_3^{(1,0)} = n_{,3}^{(1,0)}, \quad N_3^{(0,1)} = n_{,3}^{(0,1)}. \tag{33}$$

In the zeroth-order constitutive relations, the shear force resultants $T_4^{(0,0)}$ and $T_5^{(0,0)}$, which are caused by flexure, cannot be set to zero, while the other stress resultant components in Eq. (16) are null[16,18,24–25], i.e.,

$$T_1^{(0,0)} = T_2^{(0,0)} = T_6^{(0,0)} = 0. \tag{34}$$

Equation (34) is the stress relaxation condition for the zeroth-order components, in which the extension with the Poisson effect has been considered. Introducing $\alpha, \beta = 3, 4, 5$ and $\mu = 1, 2, 6$, it can be expressed as $T_\mu^{(0,0)} = 0$. Then, Eq. (13) can be rewritten as follows:

$$4abS_\alpha^{(0,0)} = s_{\alpha\beta}T_\beta^{(0,0)} + 4abe_{k\alpha}E_k^{(0,0)}. \tag{35}$$

Similarly, Eq. (35) can be expressed in an inverted form as follows:

$$T_\alpha^{(0,0)} = 4ab(\hat{c}_{\alpha\beta}S_\beta^{(0,0)} - \hat{e}_{k\alpha}E_k^{(0,0)}), \tag{36}$$

where

$$\hat{c}_{\alpha\beta} = \frac{1}{s_{\alpha\beta}}, \quad \hat{e}_{k\alpha} = \frac{e_{k\beta}}{s_{\alpha\beta}}.$$

Substituting Eq. (36) into Eqs. (14) and (15) yields

$$D_i^{(0,0)} = 4ab(\hat{e}_{i\alpha}S_\alpha^{(0,0)} - \hat{\varepsilon}_{ik}E_k^{(0,0)}), \tag{37}$$

$$J_i^{(0,0)} = 4abq(\overline{n}\mu_{ij}E_j^{(0,0)} + \mu_{ij}\overline{E}_j n^{(0,0)} - d_{ij}N_j^{(0,0)}), \tag{38}$$

where

$$\hat{\varepsilon}_{ik} = \varepsilon_{ik} - \frac{e_{i\alpha}e_{k\beta}}{s_{\alpha\beta}}.$$

In the following, the first-order constitutive relations will be introduced. The flexural deformations emerging in the x_1- and x_2-directions should be considered separately. For example, the major first-order resultant corresponding to the flexure in the x_1-direction is the bending moment $T_3^{(1,0)}$. Therefore, it is suitable that the following first-order stress resultants are set to zero[16,18,24–25]:

$$T_1^{(1,0)} = T_2^{(1,0)} = T_4^{(1,0)} = T_5^{(1,0)} = T_6^{(1,0)} = 0. \tag{39}$$

If

$$m = 1, \quad p = 0, \quad r = 1, \quad s = 0,$$

the following relations can be obtained from Eq. (7):

$$\begin{cases} A_{(1010)}S_u^{(1,0)} = s_{uv}T_v^{(1,0)} + A_{(1010)}e_{ku}E_k^{(1,0)}, \\ D_i^{(1,0)} = e_{iu}T_u^{(1,0)} + A_{(1010)}\varepsilon_{ik}E_k^{(1,0)}, \\ J_i^{(1,0)} = qA_{(1010)}(\overline{n}\mu_{ij}E_j^{(1,0)} + \mu_{ij}\overline{E}_j n^{(1,0)} - d_{ij}N_j^{(1,0)}), \end{cases} \tag{40}$$

where

$$A_{(1010)} = \frac{4}{3}a^3b.$$

Hence, the first-order constitutive relations in the x_1-direction are

$$\begin{cases} T_3^{(1,0)} = \dfrac{4}{3}a^3b(\widetilde{c}_{33}S_3^{(1,0)} - \widetilde{e}_{k3}E_k^{(1,0)}), \\ D_i^{(1,0)} = \dfrac{4}{3}a^3b(\widetilde{e}_{i3}S_3^{(1,0)} + \widetilde{\varepsilon}_{ik}E_k^{(1,0)}), \\ J_i^{(1,0)} = \dfrac{4}{3}a^3bq(\overline{n}\mu_{ij}E_j^{(1,0)} + \mu_{ij}\overline{E}_j n^{(1,0)} - d_{ij}N_j^{(1,0)}). \end{cases} \tag{41}$$

Similarly, the major first-order resultant corresponding to the flexure in the x_2-direction is the bending moment $T_3^{(0,1)}$. Therefore, the stress relaxation condition is

$$T_1^{(0,1)} = T_2^{(0,1)} = T_4^{(0,1)} = T_5^{(0,1)} = T_6^{(0,1)} = 0. \tag{42}$$

Correspondingly, the first-order constitutive relations in the x_2-direction can be obtained as follows:

$$\begin{cases} T_3^{(0,1)} = \dfrac{4}{3}ab^3(\widetilde{c}_{33}S_3^{(0,1)} - \widetilde{e}_{k3}E_k^{(0,1)}), \\ D_i^{(0,1)} = \dfrac{4}{3}ab^3(\widetilde{e}_{i3}S_3^{(0,1)} + \widetilde{\varepsilon}_{ik}E_k^{(0,1)}), \\ J_i^{(0,1)} = \dfrac{4}{3}ab^3q(\overline{n}\mu_{ij}E_j^{(0,1)} + \mu_{ij}\overline{E}_j n^{(0,1)} - d_{ij}N_j^{(0,1)}). \end{cases} \tag{43}$$

Up to now, the 1D equations have been presented in detail for the first-order theory. Totally speaking, these equations can be classified into three categories, i.e., the dynamic equilibrium equations, generalized geometric equations, and generalized constitutive equations. The dynamic equilibrium equations consist of extension (23), flexure (24) with shear deformations (25), Gauss's law of electrostatics (26), and conservation of charge (27). The generalized geometric equations include the strain-displacement relationships (28) and (29), electric field-potential function relationships (30) and (31), and the relationships (32) and (33) between the perturbation of the carrier density and its gradient. The constitutive equations contain the zeroth-order constitutive relationships (36)–(38) and the first-order constitutive relationships in the x_1- and x_2-directions (41)–(43). With successive substitutions, the governing equations (23)–(27) can be written as eleven equations containing eleven unknowns, i.e., $u_3^{(0,0)}$, $u_1^{(0,0)}$, $u_2^{(0,0)}$, $u_3^{(1,0)}$, $u_3^{(0,1)}$, $\varphi^{(0,0)}$, $\varphi^{(1,0)}$, $\varphi^{(0,1)}$, $n^{(0,0)}$, $n^{(1,0)}$, and $n^{(0,1)}$. Similarly, in order to obtain the closed-form solutions, $u_3^{(0,0)}$ or $T_3^{(0,0)}$, $u_1^{(0,0)}$ or $T_5^{(0,0)}$, $u_2^{(0,0)}$ or $T_4^{(0,0)}$, $u_3^{(1,0)}$ or $T_3^{(1,0)}$, $u_3^{(0,1)}$ or $T_3^{(0,1)}$, $\varphi^{(m,n)}$ or $D_3^{(m,n)}$, and $n^{(m,n)}$ or $(\dot{D}_3^{(m,n)} + J_3^{(m,n)})$ should be prescribed at $x_3 = \pm c$ with $(m,n) = (0,0), (1,0)$, and $(0,1)$ for mechanical and electrical boundary conditions.

4.3 Reduction to elementary flexure

As a reduction of the first-order theory, the case of elementary flexure will be given in this subsection. For the elementary flexure without shear deformations, the corresponding rotatory inertia terms $\ddot{u}_3^{(1,0)}$ and $\ddot{u}_3^{(0,1)}$ in Eq. (25) are set to be zero[22–25] so that

$$T_{33,3}^{(1,0)} - T_{13}^{(0,0)} + F_3^{(1,0)} = 0, \quad T_{33,3}^{(0,1)} - T_{23}^{(0,0)} + F_3^{(0,1)} = 0. \tag{44}$$

After eliminating $T_{13}^{(0,0)}$ and $T_{23}^{(0,0)}$, the dynamic equilibrium equations for elementary flexure can be obtained as follows:

$$T_{33,33}^{(1,0)} + F_1^{(0,0)} + F_{3,3}^{(1,0)} = 4ab\rho\ddot{u}_1^{(0,0)}, \quad T_{33,33}^{(0,1)} + F_2^{(0,0)} + F_{3,3}^{(0,1)} = 4ab\rho\ddot{u}_2^{(0,0)}. \tag{45}$$

Correspondingly, the zeroth-order flexural shear strains $S_{31}^{(0,0)}$ and $S_{32}^{(0,0)}$ should be set to be zero. Therefore,

$$S_{31}^{(0,0)} = \frac{1}{2}(u_{1,3}^{(0,0)} + u_3^{(1,0)}) = 0, \quad S_{32}^{(0,0)} = \frac{1}{2}(u_{2,3}^{(0,0)} + u_3^{(0,1)}) = 0, \tag{46}$$

$$S_{33}^{(1,0)} = -u_{1,33}^{(0,0)}, \quad S_{33}^{(0,1)} = -u_{2,33}^{(0,0)}. \tag{47}$$

Similarly, the theory of extension and elementary flexure also contains three categories of equations, i.e., the dynamic equilibrium equations, generalized geometric equations, and

generalized constitutive equations. The dynamic equilibrium equations consist of extension (23), flexure (45), Gauss's law of electrostatics (26), and conservation of charge (27). The generalized geometric equations are composed of extensional strain (28), flexural strains (47), electric field-potential function relationships (30) and (31), and the relationships (32) and (33) between the perturbation of the carrier density and its gradient relation. The constitutive equations are, respectively, the extensional constitutive relationship (36) when $\alpha = 3$, the relationship between the shear force and bending moment (44), and other constitutive relationships (37) and (38). After necessary substitutions and derivations, these equations can be simplified as nine equations with nine unknowns, i.e., $u_3^{(0,0)}$, $u_1^{(0,0)}$, $u_2^{(0,0)}$, $\varphi^{(0,0)}$, $\varphi^{(1,0)}$, $\varphi^{(0,1)}$, $n^{(0,0)}$, $n^{(1,0)}$, and $n^{(0,1)}$. Similarly, nine boundary conditions should be prescribed at $x_3 = \pm c$.

5 Static analysis of the extensional motion

As an application of the 1D equations, the static extensional motion of the piezoelectric semiconductor beam is considered firstly. Equations (20)–(22) can be reduced to

$$T_{33,3}^{(0,0)} = 0, \quad D_{3,3}^{(0,0)} = 4abqn^{(0,0)}, \quad J_{3,3}^{(0,0)} = 0. \tag{48}$$

Assuming that $E_3 = 0$ and substituting the generalized constitutive equations for the zeroth-order theory, i.e., Eqs. (17)–(19), into Eq. (48), we can get the following dynamic equilibrium equations:

$$\begin{cases} \widetilde{c}_{33} S_{3,3}^{(0,0)} - \widetilde{e}_{33} E_{3,3}^{(0,0)} = 0, \\ \widetilde{e}_{33} S_{3,3}^{(0,0)} + \widetilde{\varepsilon}_{33} E_{3,3}^{(0,0)} = q n^{(0,0)}, \\ \overline{n} \mu_{33} E_{3,3}^{(0,0)} - d_{33} n_{,33}^{(0,0)} = 0. \end{cases} \tag{49}$$

$S_3^{(0,0)}, E_3^{(0,0)}$, and $n^{(0,0)}$ can be decoupled easily from Eq. (49). Therefore,

$$n_{,33}^{(0,0)} = k^2 n^{(0,0)}, \tag{50}$$

where

$$k^2 = \frac{q\overline{n}\mu_{33}}{\kappa_{33} d_{33}}, \quad \kappa_{33} = \widetilde{\varepsilon}_{33} + \frac{\widetilde{e}_{33}^2}{\widetilde{c}_{33}}.$$

For the positive hole, i.e., $q > 0$, the solution can be obtained easily as follows:

$$n^{(0,0)} = C_1 \sinh(k x_3), \tag{51}$$

where C_1 is an undetermined coefficient, and only the symmetric mode in the x_3-direction is considered. Conversely, if the electron with $q < 0$ is considered, the second and third expressions in Eq. (49) should be rewritten as follows:

$$\widetilde{e}_{33} S_{3,3}^{(0,0)} + \widetilde{\varepsilon}_{33} E_{3,3}^{(0,0)} = -q n^{(0,0)}, \quad \overline{n} \mu_{33} E_{3,3}^{(0,0)} + d_{33} n_{,33}^{(0,0)} = 0. \tag{52}$$

Using the same procedure, the same expression as Eq. (51) can be derived. Taking the positive hole as an example, the electrical potential and displacement components are stated, respectively, as follows:

$$\varphi^{(0,0)} = -\frac{q}{k^2 \kappa_{33}} C_1 \sinh(k x_3) - C_2 x_3, \tag{53}$$

$$u_3^{(0,0)} = \frac{\widetilde{e}_{33}}{\widetilde{c}_{33}} \frac{q}{k^2 \kappa_{33}} C_1 \sinh(k x_3) + C_3 x_3, \tag{54}$$

where C_2 and C_3 are integration constants. Correspondingly,

$$\begin{cases} T_{33}^{(0,0)} = 4ab(\widetilde{c}_{33}C_3 - \widetilde{e}_{33}C_2), \\ D_3^{(0,0)} = 4ab\Big(\dfrac{q}{k}C_1\cosh(kx_3) + \widetilde{e}_{33}C_3 + \widetilde{\varepsilon}_{33}C_2\Big), \\ J_3^{(0,0)} = 4abq\overline{n}\mu_{33}C_2. \end{cases} \tag{55}$$

Only the symmetric extensional modes are considered, and the boundary condition at $x_3 = c$ (see Fig. 1) is sufficient for solving the static problem. If the symmetric deformation is caused by the carrier density perturbation n_0 at the boundary $x_3 = c$, i.e.,

$$n^{(0,0)}\Big|_{x_3=c} = n_0, \tag{56}$$

which requires

$$C_1 = \frac{n_0}{\sinh(kc)}. \tag{57}$$

(i) For the electrical open case, $D_3^{(0,0)}$ should satisfy

$$D_3^{(0,0)}\Big|_{x_3=c} = 0. \tag{58}$$

Therefore,

$$\frac{q}{k}C_1\cosh(kc) + \widetilde{e}_{33}C_3 + \widetilde{\varepsilon}_{33}C_2 = 0. \tag{59}$$

(ii) However, when the edge is electrically shorted, the electric potential equals zero, i.e.,

$$\varphi^{(0,0)}\Big|_{x_3=c} = 0. \tag{60}$$

Then, the integration constant C_2 is

$$C_2 = -\frac{qn_0}{k^2\kappa_{33}c}. \tag{61}$$

(iii) When the two ends at $x_3 = \pm c$ are free, $T_{33}^{(0,0)}$ vanishes at both ends, i.e.,

$$T_{33}^{(0,0)}\Big|_{x_3=c} = 0, \tag{62}$$

which requires

$$C_3 = \frac{\widetilde{e}_{33}}{\widetilde{c}_{33}}C_2. \tag{63}$$

In fact, it is identically zero along the whole beam.

(iv) If the end of the piezoelectric semiconductor beam is fixed at $x_3 = \pm c$, $u_3^{(0,0)}$ is confined as follows:

$$u_3^{(0,0)}\Big|_{x_3=c} = 0, \tag{64}$$

which means

$$C_3 = -\frac{\widetilde{e}_{33}}{\widetilde{c}_{33}}\frac{qn_0}{k^2\kappa_{33}c}. \tag{65}$$

In general, the boundary conditions come in four types: electrically open and free ends (OF), electrically shorted and free ends (SF), electrically open and simply supported ends (OS), and electrically shorted and simply supported ends (SS). The four cases will be discussed in detail in the following section.

For the numerical results, the parameters of the plate of ZnO beam are as follows[18,28–30]:

$$\begin{cases} \widetilde{c}_{33} = 211\,\mathrm{GPa}, \quad \widetilde{e}_{33} = 1.32\,\mathrm{C}\cdot\mathrm{m}^{-2}, \quad \widetilde{\varepsilon}_{33} = 8.85\times10^{-11}\,\mathrm{F}\cdot\mathrm{m}^{-1}, \\ \rho = 5\,700\,\mathrm{kg}\cdot\mathrm{m}^{-3}, \quad q = 1.602\times10^{-19}\,\mathrm{C}, \quad \mu_{33} = 1\,350\,\mathrm{cm}^2\cdot\mathrm{V}^{-1}\cdot\mathrm{s}^{-1}, \end{cases}$$

and $d_{33} = \mu_{33}k'T/q$, where k' is the Boltzmann constant, and $T = 300\,\mathrm{K}$ is the absolute temperature[21]. The length is 10 cm with the external n_0 fixed to $1\times10^{16}\,\mathrm{m}^{-3}$.

Figure 2 shows the static displacement distribution along the x_3-direction for different boundary conditions. The cases of SF, OS, and SS have the same displacement distribution, which can be proven from Eqs. (54), (61), (63), and (65). The amplitude of OF is smaller than those of the aforementioned three cases. The deformations are mainly focused on the end of the piezoelectric semiconductor beam. At the region of $|x_3| < 4\,\mathrm{cm}$, the displacement almost remains at zero. Meanwhile, the initial carrier density $\overline{n}$ has a significant effect on the displacement distribution (see Fig. 3). A large $\overline{n}$ leads to a small amplitude, which implies dissipation as a result of semiconduction.

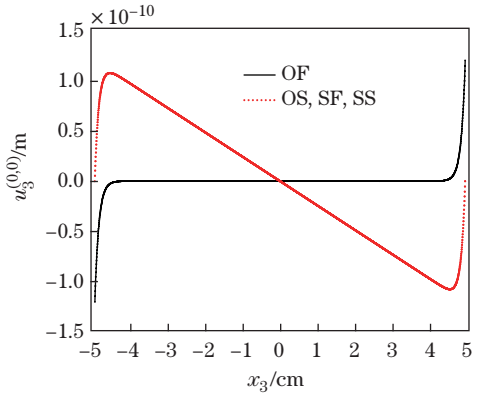

Fig. 2 Static displacement distribution along the x_3-direction for different boundary conditions

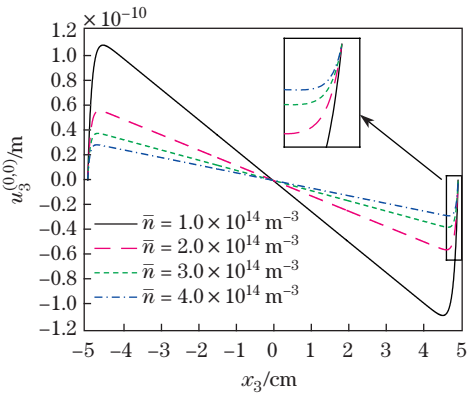

Fig. 3 Effects of the initial carrier density $\overline{n}$ on the static displacement distribution along the x_3-direction (OS condition)

6 Dynamic analysis of the extensional motion

Typically, wave devices, which are made of piezoelectric materials or semiconductors, are very small with the size on the order of centimeter, sometimes even on the order of millimeter. Investigating the dynamic properties of piezoelectric semiconductor beams seems to be more valuable. Taking the aforementioned 1D extensional motion as an example, the dynamic behavior of the piezoelectric semiconductor beam can be controlled by the following equations:

$$\begin{cases} \widetilde{c}_{33}u_{3,33}^{(0,0)} + \widetilde{e}_{33}\varphi_{,33}^{(0,0)} = \rho\ddot{u}_3^{(0,0)}, \\ \widetilde{e}_{33}u_{3,33}^{(0,0)} - \widetilde{\varepsilon}_{33}\varphi_{,33}^{(0,0)} = qn^{(0,0)}, \\ \dot{n}^{(0,0)} - \overline{n}\mu_{33}\varphi_{,33}^{(0,0)} - d_{33}n_{,33}^{(0,0)} = 0. \end{cases} \tag{66}$$

A solution of Eq. (66) can be explored as follows[30–33]:

$$u_3^{(0,0)} = A\exp(\xi x_3 + \mathrm{i}\omega t), \quad \varphi^{(0,0)} = B\exp(\xi x_3 + \mathrm{i}\omega t), \quad n^{(0,0)} = C\exp(\xi x_3 + \mathrm{i}\omega t), \tag{67}$$

where A, B, and C are undetermined constants. ξ and ω stand for the circular frequency and the wavenumber, respectively. This solution must satisfy the governing equation (66), which leads to three homogeneous linear equations for A, B, and C, i.e.,

$$\begin{cases} (\widetilde{c}_{33}\xi^2 + \rho\omega^2)A + \widetilde{e}_{33}\xi^2 B = 0, \\ \widetilde{e}_{33}\xi^2 A - \widetilde{\varepsilon}_{33}\xi^2 B - qC = 0, \\ \overline{n}\mu_{33}\xi^2 B + (d_{33}\xi^2 - \mathrm{i}\omega)C = 0. \end{cases} \tag{68}$$

For the nontrivial solutions of A, B, and C, the determinant of the coefficient matrix of Eq. (3) should be equal to zero, from which an algebraic equation about ξ can be deduced as follows:

$$\Big(-\xi^4 + \Big(\frac{\widetilde{c}_{33}}{\overline{c}_{33}}\frac{q\overline{n}\mu_{33}}{\widetilde{\varepsilon}_{33}d_{33}} - \frac{\omega^2\rho}{\overline{c}_{33}} + \frac{\mathrm{i}\omega}{d_{33}}\Big)\xi^2 + \frac{\rho\omega^2}{\overline{c}_{33}}\Big(\frac{q\overline{n}\mu_{33}}{\widetilde{\varepsilon}_{33}d_{33}} + \frac{\mathrm{i}\omega}{d_{33}}\Big)\Big)\xi^2 = 0, \tag{69}$$

where

$$\overline{c}_{33} = \frac{\widetilde{e}_{33}^2}{\widetilde{\varepsilon}_{33}^2}.$$

Equation (69) comprises six roots, i.e.,

$$\xi_{1,2} = 0, \quad \xi_{3,4} = \pm\sqrt{\frac{-B' + \sqrt{B'^2 - 4A'C'}}{2A'}}, \quad \xi_{5,6} = \pm\sqrt{\frac{-B' - \sqrt{B'^2 - 4A'C'}}{2A'}}, \tag{70}$$

where

$$A' = 1, \quad B' = \frac{\widetilde{c}_{33}}{\overline{c}_{33}}\frac{q\overline{n}\mu_{33}}{\widetilde{\varepsilon}_{33}d_{33}} - \frac{\omega^2\rho}{\overline{c}_{33}} + \frac{\mathrm{i}\omega}{d_{33}}, \quad C' = \frac{\omega^2\rho}{\overline{c}_{33}}\Big(\frac{q\overline{n}\mu_{33}}{\widetilde{\varepsilon}_{33}d_{33}} + \frac{\mathrm{i}\omega}{d_{33}}\Big). \tag{71}$$

Considering the structural and loading symmetry, only three roots are enough to construct the solution. Assume

$$\lambda_1 = \xi_1 = 0, \quad \lambda_2 = \xi_3 = \sqrt{\frac{-B' + \sqrt{B'^2 - 4A'C'}}{2A'}}, \quad \lambda_3 = \xi_5 = \sqrt{\frac{-B' - \sqrt{B'^2 - 4A'C'}}{2A'}}. \tag{72}$$

Then, Eq. (67) can be written as follows:

$$\begin{cases} u_3^{(0,0)} = \alpha_2 A_2\sinh(\lambda_2 x_3) + \alpha_3 A_3\sinh(\lambda_3 x_3), \\ \varphi^{(0,0)} = A_1 x_3 + A_2\sinh(\lambda_2 x_3) + A_3\sinh(\lambda_3 x_3), \\ n^{(0,0)} = \beta_2 A_2\sinh(\lambda_2 x_3) + \beta_3 A_3\sinh(\lambda_3 x_3), \end{cases} \tag{73}$$

where the common term of $\exp(\mathrm{i}\omega t)$ has been omitted for brevity,

$$\alpha_m = -\frac{\widetilde{e}_{33}\lambda_m^2}{\widetilde{c}_{33}\lambda_m^2 + \rho\omega^2}, \quad \beta_m = \frac{\overline{n}\mu_{33}\lambda_m^2}{\mathrm{i}\omega - d_{33}\lambda_m^2}, \quad m = 2, 3, \tag{74}$$

and A_1, A_2, and A_3 can be determined with the aid of the boundary conditions. Then, the stress resultant $T_{33}^{(0,0)}$, electric displacement resultant $D_3^{(0,0)}$, and current resultant $J_3^{(0,0)}$ can be calculated through

$$\begin{cases} T_{33}^{(0,0)} = 4ab((\widetilde{c}_{33}\alpha_2 + \widetilde{e}_{33})\lambda_2 A_2 \cosh(\lambda_2 x_3) \\ \qquad\qquad + (\widetilde{c}_{33}\alpha_3 + \widetilde{e}_{33})\lambda_3 A_3 \cosh(\lambda_3 x_3) + \widetilde{e}_{33} A_1), \\ D_3^{(0,0)} = 4ab((\widetilde{e}_{33}\alpha_2 - \widetilde{\varepsilon}_{33})\lambda_2 A_2 \cosh(\lambda_2 x_3) \\ \qquad\qquad + (\widetilde{e}_{33}\alpha_3 - \widetilde{\varepsilon}_{33})\lambda_3 A_3 \cosh(\lambda_3 x_3) - \widetilde{\varepsilon}_{33} A_1), \\ J_3^{(0,0)} = -4abq((\overline{n}\mu_{33} + d_{33}\beta_2)\lambda_2 A_2 \cosh(\lambda_2 x_3) \\ \qquad\qquad + (\overline{n}\mu_{33} + d_{33}\beta_3)\lambda_3 A_3 \cosh(\lambda_3 x_3) + \overline{n}\mu_{33} A_1). \end{cases} \tag{75}$$

Similar to the static analysis, the symmetric vibration mode is excited by the carrier density perturbation $n_0 \exp(\mathrm{i}\omega t)$ at the boundary $x_3 = c$. This boundary condition is sometimes difficult to achieve in practice. Nevertheless, investigating and understanding the effect of semiconductor properties is still important and beneficial, which can interpret the inner physical mechanism of semiconductor in piezoelectrics. Therefore,

$$\beta_2 A_2 \sinh(\lambda_2 c) + \beta_3 A_3 \sinh(\lambda_3 c) = n_0. \tag{76}$$

The boundary conditions are as follows:

(i) For the electrically open case, Eq. (58) requires

$$(\widetilde{e}_{33}\alpha_2 - \widetilde{\varepsilon}_{33})\lambda_2 A_2 \cosh(\lambda_2 c) + (\widetilde{e}_{33}\alpha_3 - \widetilde{\varepsilon}_{33})\lambda_3 A_3 \cosh(\lambda_3 c) - \widetilde{\varepsilon}_{33} A_1 = 0. \tag{77}$$

(ii) For the electrically shorted case, Eq. (60) can be reduced to

$$A_1 c + A_2 \sinh(\lambda_2 c) + A_3 \sinh(\lambda_3 c) = 0. \tag{78}$$

(iii) When the two ends at $x_3 = \pm c$ are free, Eq. (62) is equal to

$$(\widetilde{c}_{33}\alpha_2 + \widetilde{e}_{33})\lambda_2 A_2 \cosh(\lambda_2 c) + (\widetilde{c}_{33}\alpha_3 + \widetilde{e}_{33})\lambda_3 A_3 \cosh(\lambda_3 c) + \widetilde{e}_{33} A_1 = 0. \tag{79}$$

(iv) If the piezoelectric semiconductor beam is simply supported at $x_3 = \pm c$, the following relation can be obtained by use of Eq. (64):

$$\alpha_2 A_2 \sinh(\alpha_2 c) + \alpha_3 A_3 \sinh(\alpha_3 c) = 0. \tag{80}$$

The displacement signal calculated at $x_3 = 0.5c$ versus the driving frequency for different boundary conditions are shown in Fig. 4, from which we can conclude that the displacements assume their own maxima at resonant frequencies. Hence, the piezoelectric semiconductor beam can be viewed as a resonant device, which has better performance at a particular frequency[32–33]. As pointed out, the maximum amplitude of the first resonance is not shown exactly in Fig. 4. However, the first peak value is larger than the others. Actually, the corresponding modes for high resonances have nodal points along the length direction, which will lead to some voltage cancelation in a piezoelectric semiconductor beam and furthermore smaller displacement response[34]. Meanwhile, the boundary conditions have significant effects on the dynamic properties of the beam. As shown in Figs. 4(a) and 4(b), six symmetric resonances can be identified in the region of $\omega \leqslant 2.4 \times 10^6$ rad $\cdot$ s^{-1} when the ends at $x_3 = \pm c$ are free from traction. However, if the ends at $x_3 = \pm c$ are simply supported (see Fig. 4(c)), only three resonances can be observed under the same condition. Moreover, the resonance frequency of OF is larger than that of SF (see Figs. 4(a) and 4(b)).

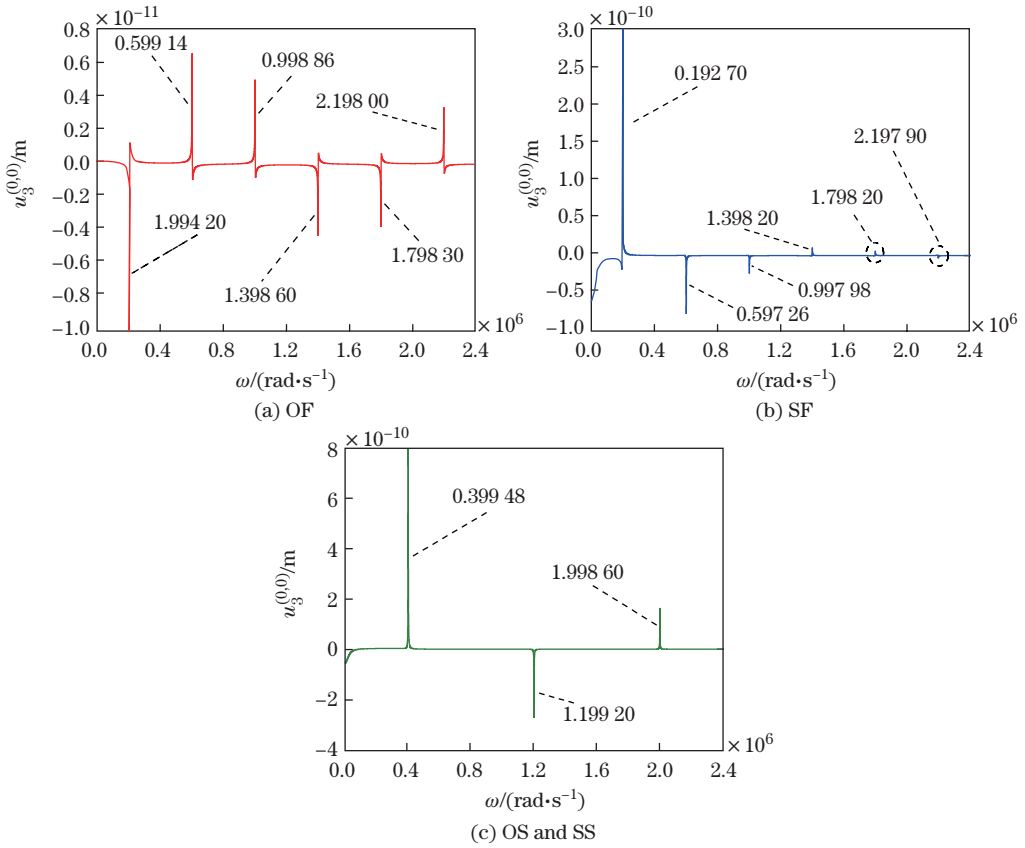

Fig. 4 Resonance of excited displacement signal at $x_3 = 0.5c$ versus the driving frequency for different boundary conditions

Actually, the length of the piezoelectric semiconductor beam will have a significant effect on the resonance frequencies. Usually, a long beam features a relatively low resonance frequency, which has been proved by Fig. 5. Fortunately, the resonance amplitude is insensitive to the length parameter (see Fig. 5). To some extent, the insensitivity is beneficial for the design of a piezoelectric semiconductor beam. The length can be chosen freely according to the external frequency of the beam, which will not reduce the displacement response.

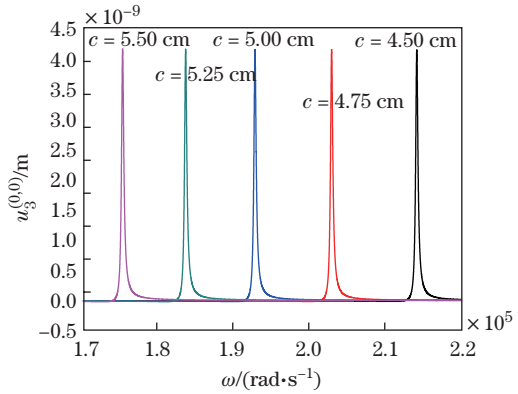

Fig. 5 Effects of c on the first resonance at $x_3 = 0.5c$ under the SF condition (color online)

As a result of the displacement signal achieving its maximum at the first resonance, the effect of the initial carrier density $\overline{n}$ on the first resonance for the extensional vibration is mainly explored in the following discussion. Both the resonant frequency and the resonance amplitude are sensitive to the initial carrier density $\overline{n}$ (see Fig. 6). A large $\overline{n}$ implies great dissipation as a result of the semiconduction, and leads to a weak resonance with a small amplitude. In order to depict the effect of the semiconduction more visually, Fig. 7 presents the variation trend of resonance frequency and resonance amplitude of the excited displacement signal at $x_3 = 0.5c$ versus the initial carrier density $\overline{n}$ when the ends at $x_3 = \pm c$ are electrically shorted and traction free. The two curves sharply decrease first and then approach some special values when $\overline{n}$ increases. The resonance amplitude of excited displacement is not zero when the initial carrier density $\overline{n} \geqslant 1 \times 10^{15}\,\mathrm{m}^{-3}$. For instance, when the initial carrier density is assumed to be $\overline{n} = 1 \times 10^{15}\,\mathrm{m}^{-3}$, the amplitude of the excited displacement is $4.12 \times 10^{-10}\,\mathrm{m}$, and when $\overline{n} = 5 \times 10^{15}\,\mathrm{m}^{-3}$, the amplitude is $8.3 \times 10^{-11}\,\mathrm{m}$. However, our results show that the corresponding displacement magnitude is $2.064 \times 10^{-8}\,\mathrm{m}$ when $\overline{n} = 2 \times 10^{13}\,\mathrm{m}^{-3}$.

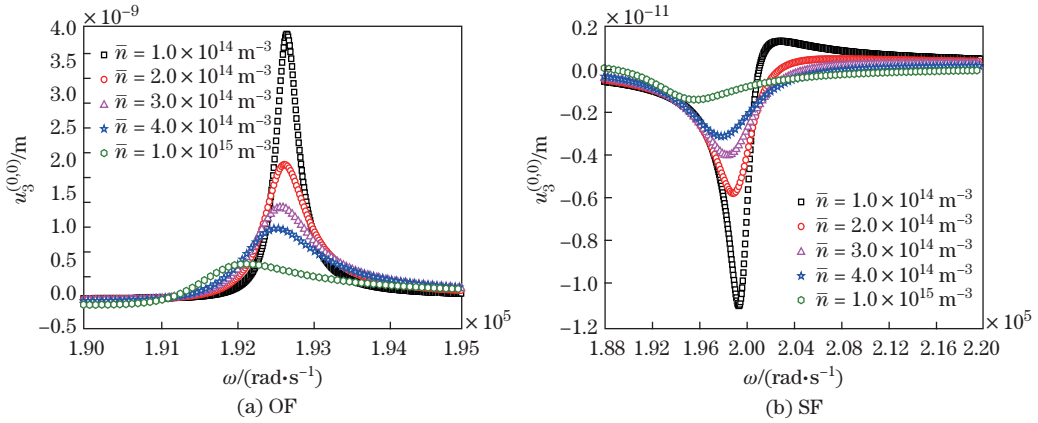

Fig. 6 Effects of $\overline{n}$ on the first resonance of the excited displacement signal at $x_3 = 0.5c$ under different boundary conditions (color online)

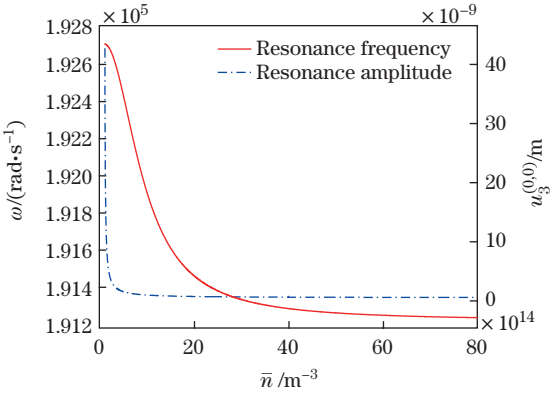

Fig. 7 Resonance frequency and amplitude of the excited displacement signal at $x_3 = 0.5c$ versus the initial carrier density $\overline{n}$ under the SF condition

7 Conclusions

Totally speaking, the reduced 1D equations of a piezoelectric semiconductor beam with a rectangular cross section are proposed with the aid of a double power series expansion tech-

nique. These equations are general and widely applicable, which can be degenerated to a number of special cases, e.g., extensional motion, coupled extensional and flexural motion with shear deformations, and elementary flexural motion without shear deformations. Based on these equations, numerical simulations are carried out sequentially to explore the effects of the semiconduction on the static deformation and dynamic extensional behaviors of a slender ZnO beam. It has been revealed that both the resonance frequency and the displacement response evidently decrease, owing to the initial carrier density existing in piezoelectric semiconductor media. The equations derived in the present contribution and the qualitative results about the semiconduction in the piezoelectrics can be viewed as the benchmark for further theoretical and experimental investigation.

References

[1] Benes, E., Groschl, M., Seifert, F., and Pohl, A. Comparison between BAW and SAW sensor principles. *IEEE Transactions on Ultrasonics, Ferroelectrics, and Frequency Control*, **45**, 1314–1330 (1998)

[2] Vellekoop, M. J. Acoustic wave sensors and their technology. *Ultrasonics*, **36**, 7–14 (1998)

[3] Wang, Q. and Varadan, V. K. Wave propagation in piezoelectric coupled plates by use of interdigital transducer, part 2: wave excitation by interdigital transducer. *International Journal of Solids and Structures*, **39**, 1131–1144 (2002)

[4] Karlash, V. L. Electroelastic vibrations and transformation ratio of a planar piezoceramic transformer. *Journal of Sound and Vibration*, **277**, 353–367 (2004)

[5] Stanton, S. C., Erturk, A., Mann, B. P., Dowell, E. H., and Inman, D. J. Nonlinear nonconservative behavior and modeling of piezoelectric energy harvesters including proof mass effects. *Journal of Intelligent Material Systems and Structures*, **23**, 183–199 (2011)

[6] Miyazaki, S. Long-term unrestrained measurement of stride length and walking velocity utilizing a piezoelectric gyroscope. *IEEE Transactions on Biomedical Engineering*, **44**, 753–759 (1997)

[7] Tomar, M., Gupta, V., Mansingh, A., and Sreenivas, K. Temperature stability of c-axis oriented $LiNbO_3/SiO_2/Si$ thin film layered structures. *Journal of Physics D: Applied Physics*, **34**, 2267–2273 (2001)

[8] Baumhauer, J. C. and Tiersten, H. F. Nonlinear electroelastic equations for small fields superposed on a bias. *The Journal of the Acoustical Society of America*, **54**, 1017–1034 (1973)

[9] Collet, B., Destrade, M., and Maugin, G. A. Bleustein-Gulyaev waves in some functionally graded materials. *European Journal of Mechanics-A/Solids*, **25**, 695–706 (2006)

[10] Nayfeh, A. H. and Nagy, P. B. Excess attenuation of leaky Lamb waves due to viscous fluid loading. *The Journal of the Acoustical Society of America*, **101**, 2649–2658 (1997)

[11] Liu, J. S. and He, S. T. Theoretical analysis on Love waves in a layered structure with a piezoelectric substrate and multiple elastic layers. *Journal of Applied Physics*, **107**, 073511 (2010)

[12] Li, P., Jin, F., and Yang, J. S. Effects of semiconduction on electromechanical energy conversion in piezoelectrics. *Smart Materials and Structures*, **24**, 025021 (2015)

[13] Tiersten, H. F. and Sham, T. L. On the necessity of including electrical conductivity in the description of piezoelectric fracture in real materials. *IEEE Transactions on Ultrasonics, Ferroelectrics, and Frequency Control*, **45**, 1–3 (1998)

[14] Yong, Y. K., Patel, M. S., and Tanaka, M. Theory and experimental verifications of the resonator Q and equivalent electrical parameters due to viscoelastic and mounting supports losses. *IEEE Transactions on Ultrasonics, Ferroelectrics, and Frequency Control*, **57**, 1831–1839 (2010)

[15] Hosseini-Hashemi, S., Salehipour, H., and Atashipour, S. R. Exact three-dimensional free vibration analysis of thick homogeneous plates coated by a functionally graded layer. *Acta Mechanica*, **223**, 2153–2166 (2012)

[16] Mindlin, R. D. High frequency vibrations of piezoelectric crystal plates. *International Journal of Solids and Structures*, **8**, 895–906 (1972)

[17] Vashishth, A. K. and Gupta, V. Vibrations of porous piezoelectric ceramic plates. *Journal of Sound and Vibration*, **325**, 781–797 (2009)

[18] Yang, J. S. and Zhou, H. G. Amplification of acoustic waves in piezoelectric semiconductor plates. *International Journal of Solids and Structures*, **42**, 3171–3183 (2005)

[19] White, D. L. Amplification of ultrasonic waves in piezoelectric semiconductors. *Journal of Applied Physics*, **33**, 2547–2554 (1962)

[20] Wauer, J. and Suherman, S. Thickness vibrations of a piezo-semiconducting plate layer. *International Journal of Engineering Science*, **35**, 1387–1404 (1997)

[21] Yang, J. S., Song, Y. C., and Soh, A. K. Analysis of a circular piezoelectric semiconductor embedded in a piezoelectric semiconductor substrate. *Archive of Applied Mechanics*, **76**, 381–390 (2006)

[22] Li, P., Jin, F., and Ma, J. X. Mechanical analysis on extensional and flexural deformations of a thermo-piezoelectric crystal beam with rectangular cross section. *European Journal of Mechanics-A/Solids*, **55**, 35–44 (2016)

[23] Dokmeci, M. C. A theory of high frequency vibrations of piezoelectric crystal bars. *International Journal of Solids and Structures*, **10**, 401–409 (1974)

[24] Yang, J. S. Equations for the extension and flexure of a piezoelectric beam with rectangular cross section and applications. *International Journal of Applied Electromagnetics and Mechanics*, **9**, 409–420 (1998)

[25] Zhang, C. L., Chen, W. Q., Li, J. Y., and Yang, J. S. One-dimensional equations for piezoelectromagnetic beams and magnetoelectric effects in fibers. *Smart Materials and Structures*, **18**, 095026 (2009)

[26] Tiersten, H. F. *Linear Piezoelectric Plate Vibrations*, Plenum Press, New York, 141–168 (1969)

[27] Mindlin, R. D. Low frequency vibrations of elastic bars. *International Journal of Solids and Structures*, **12**, 27–49 (1976)

[28] Qin, L. F., Chen, Q. M., Cheng, H. B., Chen, Q., Li, J. F., and Wang, Q. M. Viscosity sensor using ZnO and AlN thin film bulk acoustic resonators with tilted polar *c*-axis orientations. *Journal of Applied Physics*, **110**, 094511 (2011)

[29] Zhang, C. L., Wang, X. Y., Chen, W. Q., and Yang, J. S. Carrier distribution and electromechanical fields in a free piezoelectric semiconductor rod. *Journal of Zhejiang University-Science A*, **17**, 37–44 (2016)

[30] Navon, D. H. *Semiconductor Microdevices and Materials*, CBS College Publishing, New York, 416–417 (1986)

[31] Zhang, C. L., Wang, X. Y., Chen, W. Q., and Yang, J. S. An analysis of the extension of a ZnO piezoelectric semiconductor nanofiber under an axial force. *Smart Materials and Structures*, **62**, 025030 (2017)

[32] Zhao, Z. N., Qian, Z. H., Wang, B., and Yang, J. S. Analysis of thickness-shear and thickness-twist modes of AT-cut quartz acoustic wave resonator and filter. *Applied Mathematics and Mechanics* (*English Edition*), **36**(12), 1527–1538 (2015) https://doi.org/10.1007/s10483-015-2008-6

[33] Xie, X., Kong, L. C., Wang, Y. X., Zhang, J., and Hu, Y. T. Coupled vibrations and frequency shift of compound system consisting of quartz crystal resonator in thickness-shear motions and micro-beam array immersed in liquid. *Applied Mathematics and Mechanics* (*English Edition*), **36**(2), 225–232 (2015) https://doi.org/10.1007/s10483-015-1902-7

[34] Zhang, C. L., Wang, X. Y., Chen, W. Q., and Yang, J. S. Propagation of extensional waves in a piezoelectric semiconductor rod. *AIP Advances*, **6**, 045301 (2016)